

# Research Journal of Pharmaceutical, Biological and Chemical Sciences

## Biological and Thermal Investigation of Lanthanide (III) Nitrate Complexes with Schiff Base of 4-[N-(2-methoxybenzylimine) formyl] 1-2,3-dimethyl-1-phenyl-3-pyrazolin-5-one.

G Rijulal\*.

Department of Chemistry, Government College Chittur, Kerala - 678104, India.

### ABSTRACT

Thermogravimetric and biological investigations of complexes of lanthanide (III) nitrate with Schiff bases 4-[N-(2-methoxybenzylimine) formyl] 1-2,3-dimethyl-1-phenyl-3-pyrazolin-5-one (2mbfa), under the general formula  $[Ln(2mbfa)_2(NO_3)_3]$  was investigated. *Escherichia coli*, *Bacillus subtilis* and *Staphylococcus aureus* were used to test the complexes' antibacterial capabilities. According to the scientific results, every complex has more antibacterial potential than ligands. The thermogravimetric curves of all the complexes show that there are two stages of decomposition and that the final residue becomes lanthanide oxide. The Coats-Redfern equation was utilized to calculate the kinetic parameters for each thermal decomposition reaction, including the order parameter, energy of activation, pre-exponential factor, and entropy of activation. The complexes with the highest activation entropy are those that progress through the second phase of decomposition. Positive entropy of activation values imply that the decomposition products have less ordered structures than the reactants, which causes the reactions to proceed more quickly than usual. The maximum correlation coefficient values are obtained for every decomposition reaction, in accordance with the Mampel equation  $-\ln(1-\alpha)$ .

**Keywords:** Lanthanide (III) complexes, bacterial studies, antipyrine-4-carboxaldehyde, kinetic parameters.

\*Corresponding author

## INTRODUCTION

The coordination chemistry lanthanide (III) ions are rapidly expanding due to their application in biology, material science, chemistry and applied research [1]. Compared to transition elements, lanthanide ions often exhibit larger coordination numbers [2–7]. There are numerous uses for lanthanides and their Schiff base complexes in photochemistry and medicine [8]. Because of their intriguing pharmacological characteristics, antipyrine and its derivatives are employed for a variety of therapeutic objectives [9–14]. Numerous pyrazoles and their derivatives find extensive use in the field of medicine [15]. Because of their diverse range of biological applications and unique structural characteristics, lanthanide compounds containing Schiff base ligands have piqued interest [16]. Around the world, a large number of scientists and engineers employ thermal analysis in many applications and for fundamental research. Applications for thermal analysis are numerous and include minerals, inorganic materials, metals, ceramics, electronic materials, polymers, organic materials, pharmaceuticals, food, and living things [17]. Information about dehydration, thermal breakdown, adsorption, chemisorption, crystallization, melting, and crystal transition can be found by studying thermal properties, which makes them highly significant [18–23].

The Schiff base 4-N-(4'-antipyrylmethylidene)aminoantipyrine, as well as the nitrate and iodide complexes of yttrium and lanthanide with the general formulas  $[\text{Ln}(\text{AA})_2(\text{NO}_3)_2]\text{NO}_3$  and  $[\text{Ln}(\text{AA})_2\text{I}]\text{I}_2$ , were synthesized and explained. To conduct the thermogravimetric analyses, the complexes were employed. The data on thermal decomposition suggests that the nitrate complexes undergo two stages of degradation and remain stable up to 220°C. Iodide complexes also go through three stages of breakdown at 150°C. Nitrate complexes completely decompose between 800 and 850 degrees Celsius, at which point matching metal oxides are produced. Anhydrous metal iodide, the ultimate breakdown product in the case of iodide complexes, was produced after 600°C [24, 25]. Specific methods are used to produce and analyse rare earth perchlorates, which then combine to form complexes with the Schiff base 1,2-(diimino-4'-antipyrynyl)ethane. In a nitrogen environment, the complexes with the general formula  $[\text{Ln}(\text{GA})_2(\text{ClO}_4)](\text{ClO}_4)_2$  were stable for roughly 200°C. The end products were the respective anhydrous corresponding chlorides, which were obtained after two stages of breakdown at roughly 750°C [26]. The kinetic parameters of 4-N-(4'-antipyrylmethylidene)aminoantipyrine complexes of lanthanide perchlorate were calculated using the Coats-Redfern equation. It demonstrates that the ligand is only loosely attached to the metal ion and that the activated complex is more ordered than the reactants [27]. We have synthesized and studied the compounds  $[\text{Ln}(\text{FDPP})_4(\text{ClO}_4)](\text{ClO}_4)_2$  of yttrium and lanthanide perchlorates with 4-formyl-2,3-dimethyl-1-phenyl-3-pyrazoline-5-one (FDPP). The lanthanum complex, which is stable up to 210°C according to thermogravimetric analysis, proceeds through a two-stage thermal breakdown process, having anhydrous lanthanum chloride emerging as the final residue [28]. Thermogravimetry investigations of lanthanide complexes with perchlorates and iodides and N,N'-bis(4'-antipyrylmethylidene)ethylenediamine revealed that the complexes go through two stages of disintegration, with the ultimate products being corresponding anhydrous lanthanide chloride and oxides [29,30]. Utilizing Schiff base 1,2-(diimino-4'-antipyrynyl)ethane perchlorate, nitrate, and iodide complexes of lanthanum have been used to explore the kinetics and processes of each stage of thermal degradation [31]. We examined the thermal characteristics of lanthanide complexes that were produced,  $[\text{Ln}(\text{FDPP})_2(\text{NO}_3)_2]\text{NO}_3$ . According to the data, the complexes decompose in two stages at 170°C, with the ultimate result being the corresponding anhydrous lanthanide oxide [32].

The phenomenological information of 4-formyl-2,3-dimethyl-1-phenyl-3-pyrazolin-5-one lanthanum iodide complex shows that the chemical undergoes a three-stage breakdown, with lanthanum oxide emerging as the end product [33]. C.R. Vinodkumar et al. conducted a thorough analysis of the thermal properties among nitrate complexes of 4-N-(2'-furfurylidene)aminoantipyrine of lanthanide [34]. The thorium(IV) mixed ligand complexes were described by Agarwal et al. and subjected to thermal investigations [35]. The thorium(IV) complexes of 4[N-(3,4,5-trimethoxybenzalidene) amino] and 4[N-(4'-nitrobenzalidene) amino] antipyrine semicarbazone were evaluated in terms of their thermal, physicochemical, and distinctive properties [36]. 2004 saw the publication of research on thorium(IV) and dioxouranium(VI) semicarbazone complexes [37, 38]. A few compounds of lanthanide(III) chloride with isonicotinic acid and 4-amino antipyrine derivatives were investigated. After ~825°C, lanthanum(III) oxide residues are produced, and the complexes are stable up to roughly 210°C with a two-stage breakdown [39]. Comprehensive thermal investigations of thorium(IV) and dioxouranium(VI) 4[N-(2-hydroxy-1-naphthalidene)amino]antipyrinethiosemicarbazone were carried out in 2005 by R.K. Agarwal et al. [40]. Investigations were conducted on the physico-chemical and thermal properties of dioxouranium(VI) and trivalent lanthanide complexes including derivatives of diphenyl sulfoxide and

antipyrene semicarbazone [41,42]. In some complexes, the dynamics of thermal breakdown are significantly influenced by the counter anions [43, 44]. The synthesis of six and nine coordinated complexes of rare earth elements using Schiff base 4[N-(2-hydroxy-1-naphthalidene)amino]antipyrinesemicarbazone was explored [45]. For the production of seven coordinated lanthanide(III) nitrate complexes, schiff base generated from antipyrene 4-carboxaldehyde and 2-methoxy benzylamine was used [46]. PS Ajitha [47] reported on the antibacterial research of lanthanide nitrate complexes with Schiff base produced from 4-aminoantipyrene and pyridoxal. Studies on the synthesis, X-ray crystallography, and cytotoxicity of lanthanide(III) iodide with antipyrene complexes were conducted [48]. Using X-ray diffraction, thermogravimetry, and IR spectroscopy, Shulgina et al. synthesized and studied the anionic lanthanide coordination compounds of 3-methyl-4-formyl-1-phenyl-5-pyrazolone [49]. A series of Schiff bases of 4-aminoantipyrene derivatives have been tested for bactericidal and cytotoxic activities against selected bacterial strains and brine shrimp (*Artemia salina*) nauplii, respectively [50]. The present study describes the biological activities and thermal characteristics of lanthanide(III) nitrate complexes containing Schiff bases of antipyrene-4-carboxaldehyde.

## MATERIALS AND METHODS

Synthesis and characterization of ligand and lanthanide(III) nitrate complexes were carried out by reported method [46]. The invitro recognition of antibacterial activity was performed depending on the diffusion method. The TG, DTG, and DTA measurements were conducted using a Mettler Toledo STARE thermal analysis instrument in the ambient to about 800°C temperature range using a sample mass of about 3mg, a linear heating rate of 10°Cmin<sup>-1</sup>, and a dynamic air environment with a flow rate of 60 mLmin<sup>-1</sup>.

## RESULT AND DISCUSSION

### Antimicrobial Studies

The synthesized Schiff base and their corresponding Ln(III) complexes were screened for biological activity against three bacterial species *Escherichia coli*, *Bacillus subtilis*, *Staphylococcus aureus*, by disc diffusion method [51]. The results are given in Table-1, showed that all complexes exhibit high antimicrobial activities than the corresponding ligands. The higher activity of the complexes may be attributed to the properties of metal ions, the metal ion adsorbed on the cell wall of the microorganisms with blocking the protein synthesis that is an important for further growth of the microorganism, i.e., metal ions are essential for the growth-inhibitory influence.

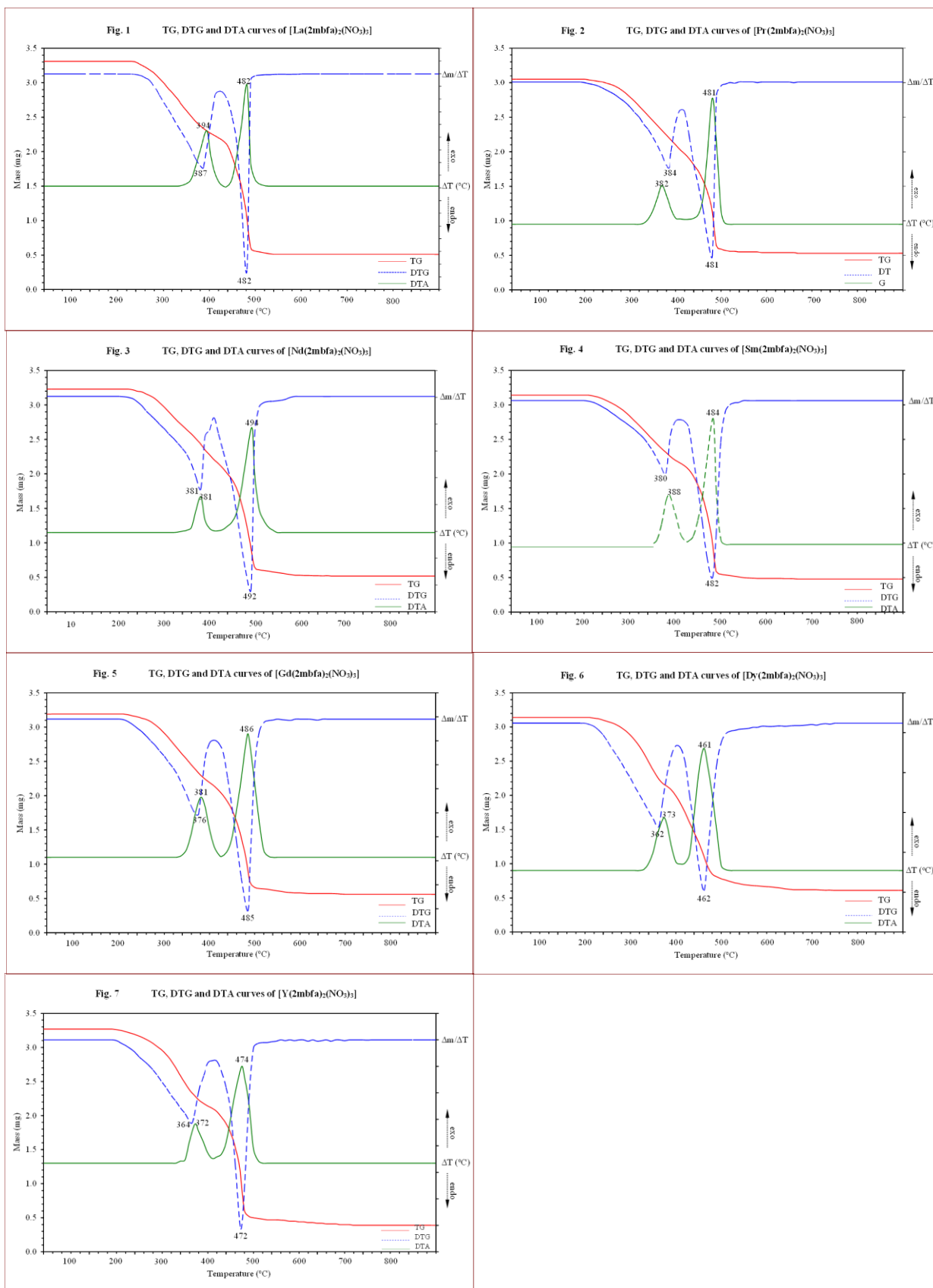
**Table 1: Antibacterial activity of ligand (3mbfa) and Ln(III) Complexes**

Compound	<i>Escherichia coli</i>	<i>Bacillus subtilis</i>	<i>Staphylococcus aureus</i>
2mbfa	+	+	+
[La(2mbfa) <sub>2</sub> (NO <sub>3</sub> ) <sub>3</sub> ]	+++	+++	+++
[Pr(2mbfa) <sub>2</sub> (NO <sub>3</sub> ) <sub>3</sub> ]	+++	+++	+++
[Nd(2mbfa) <sub>2</sub> (NO <sub>3</sub> ) <sub>3</sub> ]	++	++	+++
[Sm(2mbfa) <sub>2</sub> (NO <sub>3</sub> ) <sub>3</sub> ]	+++	++	+++
[Gd(2mbfa) <sub>2</sub> (NO <sub>3</sub> ) <sub>3</sub> ]	+++	++	++
[Dy(2mbfa) <sub>2</sub> (NO <sub>3</sub> ) <sub>3</sub> ]	++	+++	++
[Y(2mbfa) <sub>2</sub> (NO <sub>3</sub> ) <sub>3</sub> ]	++	+++	++

slightly active = +, moderately active = ++, highly active = +++

**Thermal analysis**

The thermogravimetric analysis of the lanthanide(III) nitrate complexes with 2mbfa were recorded in dynamic air at a heating rate of  $10^{\circ}\text{C min}^{-1}$  and are presented in Figs 1-7.



## Phenomenological studies

The TG curves of  $[\text{La}(\text{2mbfa})_2(\text{NO}_3)_3]$  show that the complex is stable up to  $\sim 230^\circ\text{C}$ , and then it undergoes decomposition in two stages with the completion of the decomposition at  $\sim 540^\circ\text{C}$ . These two decomposition stages are indicated by the DTG peaks at  $387$  and  $482^\circ\text{C}$ , and the corresponding DTA peaks at  $394$  and  $482^\circ\text{C}$ . The first decomposition stage starts at  $270^\circ\text{C}$  and ends at  $430^\circ\text{C}$  with a mass loss of  $33.9\%$  observed in the TG curve indicating that one of the two ligand molecules is eliminated as evidenced by the calculated mass loss value ( $33.7\%$ ). In the second stage, the decomposition begins at  $440^\circ\text{C}$  and ends at  $520^\circ\text{C}$ . The total mass loss observed in the TG curve ( $84.1\%$ ) is in agreement with the mass loss obtained from the pyrolysis experiment ( $83.2\%$ ) and the calculated mass loss value ( $83.6\%$ ). The praseodymium(III) nitrate complex with 2mbfa is stable up to  $\sim 220^\circ\text{C}$ , and thereafter, it undergoes decomposition in two stages as denoted by the DTG peaks at  $382$  and  $481^\circ\text{C}$ , and the corresponding DTA peaks at  $382$  and  $481^\circ\text{C}$ . In this complex also, one ligand molecule is removed in each step. The DTG peak widths for the first and second decomposition stages are  $270 - 440^\circ\text{C}$  and  $440 - 510^\circ\text{C}$ , respectively indicating that there is no stability region in between the two decomposition stages. The mass loss data for the first decomposition stage from the TG curve ( $33.4\%$ ) is in agreement with the calculated mass loss value for the removal of one 2mbfa molecule ( $33.6\%$ ). The final decomposition residue obtained after  $\sim 510^\circ\text{C}$  is  $\text{Pr}_6\text{O}_{11}$  in conformity with the mass loss data obtained from the TG curve ( $82.9\%$ ), pyrolysis experiment ( $84.2\%$ ) and the calculated mass loss value ( $82.9\%$ ). The complex  $[\text{Nd}(\text{2mbfa})_2(\text{NO}_3)_3]$  is stable up to  $\sim 220^\circ\text{C}$ , and then, it decomposes in two stages as indicated by the DTG peaks at  $381$  and  $492^\circ\text{C}$ , and the corresponding DTA peaks at  $381$  and  $494^\circ\text{C}$ . The first decomposition stage starts at  $280^\circ\text{C}$  and ends at  $420^\circ\text{C}$  with a mass loss of  $33.4\%$  from the TG curve. This mass loss value agrees with the calculate value for the removal of one ligand molecule ( $33.5\%$ ). The second stage decomposition reaction starts at  $430^\circ\text{C}$  and ends at  $520^\circ\text{C}$ . The total mass loss data obtained from the TG curve ( $83.6\%$ ) and the pyrolysis experiment ( $83.3\%$ ) agree with the calculated mass loss value ( $83.2\%$ ) for the formation of  $\text{Nd}_2\text{O}_3$  as the final residue. The TG curve of  $[\text{Sm}(\text{2mbfa})_2(\text{NO}_3)_3]$  complex shows that this complex is stable up to  $\sim 210^\circ\text{C}$ , and then it undergoes decomposition in two stages, which are denoted by the DTG peaks at  $380$  and  $482^\circ\text{C}$ , and the corresponding DTA peaks at  $388$  and  $484^\circ\text{C}$ . As in the cases of above complexes, this complex also eliminates one molecule of the ligand from the initial compound in the first decomposition stage. The mass loss observed in the TG curve for the first decomposition stage ( $32.8\%$ ) agrees with calculated mass loss value for the removal of one ligand molecule ( $33.3\%$ ). The decomposition of the complex is complete after  $\sim 580^\circ\text{C}$  and the entire mass loss for the thermal decomposition of the samarium complex is  $84.3\%$ . The total mass loss values obtained from the pyrolysis experiment ( $83.3\%$ ) and the calculated mass loss ( $82.7\%$ ) support the formation of  $\text{Sm}_2\text{O}_3$  as the final decomposition residue. The complex  $[\text{Gd}(\text{2mbfa})_2(\text{NO}_3)_3]$  is stable up to  $\sim 210^\circ\text{C}$ , and thereafter, it decomposes in two stages as denoted by the DTG peaks at  $376$  and  $485^\circ\text{C}$ , and the corresponding DTA peaks at  $381$  and  $486^\circ\text{C}$ . The DTG peak widths for the decomposition stages are  $250 - 410^\circ\text{C}$  and  $420 - 510^\circ\text{C}$ , respectively. The mass loss data obtained from the TG curve for the first and second decomposition stages are  $33.5\%$  and  $81.5\%$ , respectively. These mass loss values agree with the calculated mass loss values ( $33.1\%$  and  $82.1\%$ ). The final mass loss obtained from the pyrolysis experiment ( $82.6\%$ ) is also in agreement with the total mass loss for the complex with the formation of  $\text{Gd}_2\text{O}_3$  as the final residue. The complex,  $[\text{Dy}(\text{2mbfa})_2(\text{NO}_3)_3]$  shows a stability up to  $\sim 210^\circ\text{C}$ , and then it decomposes in two stages as indicated by the DTG peaks at  $362$  and  $462^\circ\text{C}$ , and the corresponding DTA peaks at  $373$  and  $461^\circ\text{C}$ . The first decomposition starts at  $240^\circ\text{C}$  and ends at  $420^\circ\text{C}$ , and the mass loss data obtained from the TG curve ( $31.7\%$ ) and the calculated value ( $32.9\%$ ) suggest that one of the two ligand molecules is eliminated from the initial compound. The second stage decomposition reaction completes after  $\sim 660^\circ\text{C}$  with a total mass loss observed in the TG curve as  $80.3\%$ . The total mass loss obtained from the pyrolysis experiment ( $81.1\%$ ) and calculated mass loss value ( $81.7\%$ ) suggest the formation of  $\text{Dy}_2\text{O}_3$  as the final residue. The TG curve of the yttrium(III) nitrate complex shows stability up to  $\sim 200^\circ\text{C}$ , and thereafter, it undergoes a two stage decomposition and the reaction ends after  $\sim 690^\circ\text{C}$ . The two decomposition stages are denoted by the DTG peaks at  $364^\circ\text{C}$  and  $472^\circ\text{C}$ , and the corresponding exothermic DTA peaks at  $372^\circ\text{C}$  and  $474^\circ\text{C}$ . The DTG peak widths for the first and the second decomposition stages are in the ranges of  $280 - 420^\circ\text{C}$  and  $430 - 510^\circ\text{C}$ , respectively. The mass loss data obtained from the TG curve ( $36.3\%$  and  $88.0\%$ ) are in agreement with the calculated mass loss values for the removal of one ligand molecule in each step ( $35.5\%$  and  $88.1\%$ ). The total mass loss obtained from the pyrolysis experiment ( $86.8\%$ ) also supports the formation of  $\text{Y}_2\text{O}_3$  as the final decomposition product.

The phenomenological data of the lanthanide(III) nitrate complexes with 2mbfa reveal that all the complexes undergo two stage thermal decomposition. In the first decomposition stage one of the 2mbfa molecules is eliminated from the initial compound. The remaining ligand molecule and the nitrate ions are

removed in the second decomposition stage with the formation of the corresponding lanthanide(III) oxides,  $\text{Ln}_2\text{O}_3$ . The lanthanum(III) nitrate complexes with 2mbfa have the maximum stability (up to  $\sim 230^\circ\text{C}$ ), while the yttrium(III) complex shows the least stability (up to  $\sim 200^\circ\text{C}$ ).

**Table 2: Phenomenological data of lanthanide(III) nitrate complexes of 2mbfa**

Compounds	Stage	Plateau in TG	DTG Peak( $^\circ\text{C}$ )	DTA Peak( $^\circ\text{C}$ )	Mass loss(%)			Assignments
					TG	Pyrol*	Calc.**	
[La(2mbfa) $_2$ (NO $_3$ ) $_3$ ]	I	Upto 230	387	394	33.9	--	33.7	Loss of one (2mbfa) Final residue La $_2$ O $_3$
	II	After 540	482	482	84.1	83.2	83.6	
[Pr(2mbfa) $_2$ (NO $_3$ ) $_3$ ]	I	Upto 280	382	382	33.4	--	33.6	Loss of one (2mbfa) Final residue Pr $_6$ O $_{11}$
	II	After 590	481	481	82.9	84.2	82.9	
[Nd(2mbfa) $_2$ (NO $_3$ ) $_3$ ]	I	Upto 220	381	381	33.4	--	33.5	Loss of one (2mbfa) Final residue Nd $_2$ O $_3$
	II	After 670	492	494	83.6	83.3	83.2	
[Sm(2mbfa) $_2$ (NO $_3$ ) $_3$ ]	I	Upto 210	380	388	32.8	--	33.3	Loss of one (2mbfa) Final residue Sm $_2$ O $_3$
	II	After 580	482	484	84.3	83.3	82.7	
[Gd(2mbfa) $_2$ (NO $_3$ ) $_3$ ]	I	Upto 210	376	381	33.5	--	33.1	Loss of one (2mbfa) Final residue Gd $_2$ O $_3$
	II	After 600	485	486	81.5	82.6	82.1	
[Dy(2mbfa) $_2$ (NO $_3$ ) $_3$ ]	I	Upto 210	362	373	31.7	--	32.9	Loss of one (2mbfa) Final residue Dy $_2$ O $_3$
	II	After 660	462	461	80.3	81.1	81.7	
[Y(2mbfa) $_2$ (NO $_3$ ) $_3$ ]	I	Upto 200	364	372	36.3	--	35.5	Loss of one (2mbfa) Final residue Y $_2$ O $_3$
	II	After 690	472	474	88.0	86.8	88.1	

\* Pyrolysis; \*\*Calculated

### Kinetic studies

The kinetic parameters such as order parameter, energy of activation, pre-exponential factor and entropy of activation for all the two decomposition stages of each of the complexes have been evaluated [52] and are presented in Table 3. The values of order parameter for the thermal decomposition reactions range from 1.0-2.2. The lowest value of order parameter is for the second decomposition stage of the yttrium(III) nitrate complex (1.0), and the highest value for the second decomposition stage of the neodymium(III) nitrate complex and the first decomposition stage of samarium(III) nitrate complex (2.2). The energy of activation (E) for the first decomposition stages of all the complexes are found to be in the range of 265.0 - 328.0  $\text{kJmol}^{-1}$  and for the second stage decomposition reactions are in the range of 308.4 - 455.7  $\text{kJmol}^{-1}$ . The pre-exponential factor (A) for the first and the second decomposition stages are in the ranges of  $1.2 \times 10^{17}$ -  $1.5 \times 10^{24}$   $\text{s}^{-1}$  and  $3.3 \times 10^{19}$ -  $6.6 \times 10^{30}$   $\text{s}^{-1}$ , respectively. The values of entropy of activation for the first and second decomposition stages are in the ranges of 74.8-211 and 121.1-337.7  $\text{JK}^{-1}\text{mol}^{-1}$ , respectively. The mechanism of the decomposition reactions of each of the stages was calculated using the different mechanistic equations suggested by Satava. The highest values of correlation coefficient for both the decomposition stages are for the Mampel equation  $-\ln(1-\alpha)$ .

**Table 3: Kinetic parameters of lanthanide(III) nitrate complexes of 2mbfa**

Compounds	Stage	Order (n)	E (kJmol <sup>-1</sup> )	A (s <sup>-1</sup> )	ΔS (JK <sup>-1</sup> mol <sup>-1</sup> )
[La(2mbfa) <sub>2</sub> (NO <sub>3</sub> ) <sub>3</sub> ]	I	1.8	315.3	5.9 × 10 <sup>22</sup>	184.4
	II	2.1	421.5	2.6 × 10 <sup>27</sup>	272.1
[Pr(2mbfa) <sub>2</sub> (NO <sub>3</sub> ) <sub>3</sub> ]	I	1.1	257.8	1.2 × 10 <sup>17</sup>	74.8
	II	1.9	447.8	1.8 × 10 <sup>29</sup>	307.4
[Nd(2mbfa) <sub>2</sub> (NO <sub>3</sub> ) <sub>3</sub> ]	I	1.8	316.8	1.9 × 10 <sup>23</sup>	194.3
	II	2.2	448.4	1.6 × 10 <sup>29</sup>	306.2
[Sm(2mbfa) <sub>2</sub> (NO <sub>3</sub> ) <sub>3</sub> ]	I	2.2	291.3	3.3 × 10 <sup>21</sup>	160.4
	II	1.6	375.6	2.0 × 10 <sup>24</sup>	212.5
[Gd(2mbfa) <sub>2</sub> (NO <sub>3</sub> ) <sub>3</sub> ]	I	1.8	328.0	1.5 × 10 <sup>24</sup>	211.6
	II	1.2	308.4	3.3 × 10 <sup>19</sup>	121.1
[Dy(2mbfa) <sub>2</sub> (NO <sub>3</sub> ) <sub>3</sub> ]	I	1.8	317.7	4.3 × 10 <sup>22</sup>	181.5
	II	1.4	455.7	6.6 × 10 <sup>30</sup>	337.7
[Y(2mbfa) <sub>2</sub> (NO <sub>3</sub> ) <sub>3</sub> ]	I	2.0	264.99	4.6 × 10 <sup>19</sup>	125.1
	II	1.0	347.54	1.9 × 10 <sup>22</sup>	174.1

### CONCLUSION

The antibacterial activity against three bacterial species *Escherichia coli*, *Bacillus subtilis*, *Staphylococcus aureus*, imply that all complexes exhibit high antimicrobial activities than the corresponding ligands. The higher activity of the complexes may be attributed to the properties of metal ions, the metal ion adsorbed on the cell wall of the microorganisms with blocking the protein synthesis that is an important for further growth of the microorganism, i.e., metal ions are essential for the growth-inhibitory influence. All the 7 complexes undergo two stage thermal decomposition. In the first decomposition stage one of the 2mbfa molecules is eliminated from the initial compound. The remaining ligand molecule and the nitrate ions are removed in the second decomposition stage with the formation of the corresponding lanthanide(III) oxides. The lanthanum(III) nitrate complexes with 2mbfa have the maximum stability (up to ~230°C), while the yttrium(III) complex shows the least stability (up to ~200°C). The values of entropy of activation for the first and second decomposition stages are in the ranges of 74.8-211 and 121.1-337.7 JK<sup>-1</sup>mol<sup>-1</sup>. The increased values of entropy of activation for the second decomposition stages for all the complexes are probably due to the less steric strain for the intermediate compounds formed after losing one molecule of ligand after the first stage decomposition. However, positive values of entropy of activation are obtained in all the decomposition stages of all the complexes indicating that the decomposition products have less ordered structures than the reactants and hence, the decomposition reactions proceed faster than normal. The mechanism of the decomposition reactions of each of the stages was calculated using the different mechanistic equations suggested by Satava. The highest values of correlation coefficient for both the decomposition stages are for the Mampel equation  $-\ln(1-\alpha)$ . Hence, these complexes follow thermal decomposition mechanism of random nucleation with one nucleus on each particle.

## REFERENCES

- [1] Atwood DA. The Rare Earth Elements: Fundamentals and Applications. John Wiley & Sons, Hoboken, New Jersey, US, 2013.
- [2] Agarwal RK, Agarwal H. Bulletin of the Chemical Society of Ethiopia 2000; 14(2): 143-154.
- [3] Agarwal RK, Chakraborti I, Agarwal H. Synthesis and Reactivity in Inorganic and Metal-Organic Chemistry 2004; 34(8): 1431-1452.
- [4] Agarwal RK, Garg R, Sindhu SK. Bulletin of the Chemical Society of Ethiopia 2005; 19(2): 185-195.
- [5] Kremer C, Torres J, Dominguez S, Mederos A. Coordination Chemistry Reviews. 2005; 249: 567-590.
- [6] Cotton S. Lanthanide and Actinide Chemistry: Inorganic Chemistry - A Text Book Series. Wiley Publication, 2006.
- [7] Agarwal RK, Prasad S, Chand V. International Journal of Chemistry 2012; 1(4): 576-597.
- [8] Alghool S, Zoromba MS, Abd El-Halim HF. Journal of Rare Earths 2013; 31(7): 715-721.
- [9] Agarwal RK, Agarwal H. Revue Roumaine de Chimie 2002; 47(5):451-454.
- [10] Madhu NT, Radhakrishnan PK, Grunert M, Weinberger P, Linert W. Reviews in Inorganic Chemistry 2003; 3(1): 1-23.
- [11] Raman N, Kulandaisamy A, Thangaraja C. Transition Metal Chemistry 2004; 29: 129-135.
- [12] Agarwal RK, Sharma D, Singh L, Agarwal H. Reviews in Inorganic Chemistry 2007; 27(1): 35-51.
- [13] Gudasi KB, Havanur VC, Patil SA, Patil BR. Metal Based Drugs 2007; 1-7.
- [14] Agarwal RK, Singh L, Sharma D. Reviews in Inorganic Chemistry 2008; 28(3): 161-181.
- [15] Delgado JN, Remers WA, Textbook of Organic Medicinal and Pharmaceutical Chemistry. Williams and Wilkins, USA, 10<sup>th</sup> edition, 1998, pp. 722-723.
- [16] Song YM, Xu JP, Ding L, Hou Q, Liu JW, Zhu ZL. J. Inorg. Biochem 2009; 103: 396-400
- [17] Ozawa T. Thermochim Acta 2000; 355: 35-42.
- [18] Vyazovkin S. Anal Chem 2002; 74(12): 2749-2762.
- [19] Dollimore D, Phang P. Anal Chem 2000; 72(12): 27-36.
- [20] Gallagher PK, Blaine R, Charsley EL, Koga N, Ozao R, Sato H, Sauerbrunn S, Schultze D, Yoshida H. J Therm Anal Calorim 2003; 72(3): 1109-1116.
- [21] Tanaka H, Brown ME. J Therm Anal Calorim 2005; 80(3): 795-797.
- [22] Criado JM, Maqueda LAP. J Therm Anal Calorim 2005; 80(1): 27-33.
- [23] L'vov BV. J Therm Anal Calorim 2005; 79(1): 151-156.
- [24] Nair MKM, Radhakrishnan PK. Polyhedron 1993; 12(10): 1227-1230.
- [25] Nair MKM, Radhakrishnan PK. Synthesis and Reactivity in Inorganic and Metal-Organic Chemistry 1996; 26(3): 529-541.
- [26] Nair MKM, Radhakrishnan PK. Synthesis and Reactivity in Inorganic and Metal-Organic Chemistry 1995; 25(1): 057-070.
- [27] Nair MKM, Radhakrishnan PK. Thermochimica Acta 1997; 292(1-2): 115-122.
- [28] Joseph S, Nair MKM, Radhakrishnan PK. Synthesis and Reactivity in Inorganic and Metal-Organic Chemistry 1997; 27(7): 1025-1038.
- [29] Joseph S, Radhakrishnan PK. Synthesis and Reactivity in Inorganic and Metal-Organic Chemistry 1998; 28(3): 423-435.
- [30] Joseph S, Radhakrishnan PK. Polyhedron 1999; 18(13): 1881-1884.
- [31] Nair MKM, Radhakrishnan PK. J Therm Anal Calorim 1998; 52(2): 475-480.
- [32] Joseph S, Radhakrishnan PK. Synthesis and Reactivity in Inorganic and Metal-Organic Chemistry 1999; 29(6): 1077-1089.
- [33] Joseph S, Radhakrishnan PK. Synthesis and Reactivity in Inorganic and Metal-Organic Chemistry 1999; 29(7): 1219-1229.
- [34] Vinodkumar CR, Nair MKM, Radhakrishnan PK. J Therm Anal Calorim 2000; 61(1): 143-149.
- [35] Agarwal RK, Chakraborti I, Sharma NK. Oriental Journal of Chemistry 2003; 19(1): 4.
- [36] Agarwal RK, Chakraborti I. Oriental Journal of Chemistry, 2003; 19(2): 13.
- [37] Agarwal RK, Chakraborti I, Agarwal H. Synthesis and Reactivity in Inorganic and Metal-Organic Chemistry 2004; 34(8): 1431-1452.
- [38] Agarwal RK, Chakraborti I, Agarwal H. Synthesis and Reactivity in Inorganic and Metal-Organic Chemistry 2004; 34(8): 1453-1470.
- [39] Agarwal RK, Prasad S, Goel N. Turkish Journal of Chemistry 2004; 28(4): 405-414.
- [40] Agarwal RK, Garg R, Sindhu SK. The Bulletin of the Chemical Society of Ethiopia 2005; 19(2): 185-195.
- [41] Agarwal RK, Prasad S. Turkish Journal of Chemistry 2006; 30(5): 553-562.



- [42] Agarwal RK, Prakash B, Kumar V, Khan AA. *Journal of the Iranian Chemical Society* 2007; 4: 114-125.
- [43] Madhu NT, Radhakrishnan PK, Linert W. *J Therm Anal Calorim* 2006; 84(3): 607-611.
- [44] Madhu NT, Radhakrishnan PK, Linert W. *International Journal of Chemical Kinetics* 2007; 39(2): 53-58.
- [45] Agarwal RK, Prasad S, Garg R Sidhu SK. *Bull Chem Soc Ethiop* 2006; 20(1): 167-172.
- [46] Rijulal G, Indrasenan P. *Journal of Rare Earths* 2007; 25(6): 670-673.
- [47] Ajitha PS, Nair MKM. *Research Journal of Pharmaceutical, Biological and Chemical Sciences* 2010; 1(4): 449-459.
- [48] Rukk NS, Albov DV, Shamsiev RS, Mudretsova SN, Davydova GA, Sadikov GG, Antsyshkina AS, Kravchenko VV, Skryabina AY, Apyrshko GN, Zamalyutin VV, Mironova EA. *Polyhedron* 2012; 44(1): 124-132.
- [49] Shulgina VF, Abkhairovaa SV, Konnika OV, Meshkovab SB, Topilovab ZM, Rusanovc EB, Aleksandrovd GG, Eremenkod IL. *Russian Journal of Inorganic Chemistry* 2013; 58(6): 678-683.
- [50] Alam MS, Lee DU, Bari ML. *J Korean Soc Appl Biol Chem* 2014; 57(5): 613-619.
- [51] Atta-ur-Rahman, Choudhary MI, Thomsen WJ. *Bioassay Techniques for Drug Development*. The Netherlands, Harwood Academic Publishers, 2001, pp.142-143.
- [52] A.W. Coats and J.P. Redfern, *Nature* 1964; 201: 68-69.
- [53] Mathew S, Nair CGR, Ninan KN. *Thermochim. Acta* 1989; 144(1): 33-43.